# Dielectric and Mechanical Relaxation in the Blends of a Polymer Liquid Crystal with Polycarbonate

**Hans-Eckart Carius and Andreas Schönhals**

*Institut für Angewandte Chemie Berlin-Adlershof, D-12484 Berlin, Germany*

**Delphine Guigner and Tomasz Sterzynski**

*Ecole Europeénne de Chimie des Polymères at des Matériaux, Université Louis Pasteur, F-67000 Strasbourg, France*

**Witold Brostow***

*Departments of Materials Science and Chemistry, University of North Texas, Denton, Texas 76203-5308*

*Received November 16, 1995*[⊗]

ABSTRACT: Bisphenol A polycarbonate (PC) and PET/0.6PHB polymer liquid crystal (PLC), where PET is poly(ethylene terephthalate), PHB is *p*-hydroxybenzoic acid, and 0.6 is the mole fraction of PHB in the copolymer, were studied along with their blends from the PC side up to 20 wt % PLC. Dielectric relaxation in the range $10^{-2}$−$10^{6}$ Hz and dynamic mechanical behavior at 1.0 Hz were determined, both as a function of temperature $T$. Broad relaxations ($\beta$ of PC, $\beta$ of the PLC), seen by earlier investigators who covered narrower frequency ranges, result in fact each from two or three distinct processes. Earlier assignments of the main $\beta$ peak of PC are discussed and found to contain a common denominator. The results are interpreted in terms of multiphase hierarchical structures contributed by the PLC related to the morphology as a function of composition and the macromolecular dynamics of the blend components. As compared to pure PET, copolymerization with PHB results in competition of increased chain stiffness with plasticization resulting from added free volume. Pertubations in the structure of the PC matrix increase up to 15 wt % of the PLC, but then they decrease because of crossing the $\theta_{\text{LC limit}}$ at which islands of the LC-rich (PHB-rich) phase separate from the matrix; the effect is seen in several properties, both mechanical and dielectric.

## Introduction and Scope

While studies of viscoelasticity have a long history,[1] the claim that we understand relaxations in polymeric materials well would be too optimistic. However, for both fundamental and practical reasons, there is now an increasing interest in heterogeneous polymers[2] such those containing fillers—and also in polymer liquid crystals (PLCs) with which we deal in this paper. PLC macromolecules typically consist of flexible sequences along with LC sequences. The latter tend to form a LC-rich phase, a fact established first by Menczel and Wunderlich,[3,4] using differential scanning calorimetry (DSC), and confirmed later by other techniques including scanning electron microscopy (SEM) where LC-rich islands were clearly visible.[5] The multiphasicity of PLC systems provides for interesting relaxational behavior.

A significant part of our understanding of PLCs comes from statistical mechanics, in particular from the Flory theory and its amplifications.[6−13] The theory involves the average fraction $\theta$ of LC sequences in the chains, the average length $\eta$ of the LC sequence, and the order parameter $s$ and makes possible prediction of the clearing temperature $T_{\text{LC−iso}}$ as a function of $\theta$. For ternary systems of the type PLC + EP + solvent, where EP is a flexible polymer, calculations based on the theory show that the LC sequences cause *channeling* of the solvent molecules.[12] Thus, imparting of the LC orientation to non-LC constituents of the system is a factor that needs to be taken into account. Structures of PLCs are hierarchical in nature.[14−17] In general, hierarchical structures can be formed if there are at least two kinds of building blocks which are *not* homeomorphic to each other.[17] With the exception of chains that do not contain flexible sequences, all other PLCs fulfill that condition. Some rules pertaining to hierarchical structures, dealing in particular with ascensions and descensions in the hierarchy, have been formulated in terms of homeomorphism.[17] The lack of homeomorphism between two figures can be established by a number of criteria, such as a difference in the number of connected components of the figures or a difference in the number of separating points.

Useful insights into relaxation phenomena can been also provided by molecular dynamics (MD) simulations. Thus, Tiller[18] used MD to simulate dielectric relaxation of several polymer structures. He observed several types of motions, including springlike (expansion and compression) as well as wavelike. He pointed out that MD provides information about different types of motions as well as about relationships between different motions. MD simulations of stress relaxation[19−21] show the collective character of the relaxation process; polymer chain segments relax in clusters rather than individually, thus confirming an earlier theory[22,23] of Bose−Einstein-like stress relaxation. However, simulations by MD just mentioned were made for non-LC polymers. There is one report of MD simulation of PLCs,[24] namely, longitudinal ones, that is with LC sequences in the main chain oriented along the chain direction.[25,26] The chains had carbon-like backbones to which tensile deformations were applied.[24] The results at lower stresses show relaxation by conversion from *trans* to *cis* conformations. Larger stresses result in crack propagation and failure—with the material strength strongly dependent on the *spatial distribution* of the LC islands, in addition to the naturally expected depen-

[⊗] Abstract published in *Advance ACS Abstracts,* June 1, 1996.

S0024-9297(95)01706-2 CCC: $12.00 

dence on the LC concentration $\theta$ and temperature $T$.

Experimental studies of PLCs are numerous. Hudson, and co-workers[27−30] used transmission electron microscopy (TEM), polarized optical microscopy (POM), wide-angle X-ray, and electron diffraction. Hudson et al. showed in some cases formation of smectic phases in addition to nematic, including smectic phases in which *the layers rather than the molecules* are aligned. They also observed significant differences between PLCs and MLCs (monomer liquid crystals, the terminology of Samulski[31]) during crystallization. On the macroscopic scale, we also have the well-known skin-core effect.[29,32] Cheng and co-workers[33] studied poly(azomethines), which are logitudinal PLCs, varying the length of the flexible sequences (spacers) in the backbone. They have found *pre*glass transitions, attributed to the spacers, and with the transition temperatures dependent on the spacer length. Springer and coworkers studied PLC combs. They have found polymorphism of LC phases[34,35] and also formation of metastable but reproducible LC phases.[36] These as well as other results demonstrate the complexity of PLC systems—but also capabilities for establishing molecular structure—property relationships.

Another experimental approach in dealing with complex polymer structure consists in studying binary blends with low concentration of one of the components. As argued by Surovtsev and his co-workers,[37] the minor component acts as a modifying agent for the polymer matrix. Relaxational behavior can then be studied in terms of the perturbation of the structure and properties of the matrix component—an approach we shall use below.

We believe that the hierarchical structures of PLCs can only be understood on the basis of concomitant theoretical, simulational, and experimental effort. Each of these approaches has its limitations. To give just one example, the MD simulation of dielectric relaxation[18] is up to now limited to frequencies $10^9$ Hz $< f < 10^{13}$ Hz; it has not been applied yet to PLC systems. Under the circumstances, we have decided to extend the base for understanding relaxation phenomena in PLCs by conducting dielectric and dynamic mechanical experiments. In both methods, varying the frequency of the probing field provides a capability for separation of relaxation modes. Moreover, different force fields are imposed in the two methods.

The choice of the system was dictated by the above considerations: a PLC, an EP, and EP + PLC blends from the EP side, so that perturbations of EP relaxation could be studied following the approach of Surovtsev and his colleagues. At the same time, addition of a PLC to an EP is known to improve mechanical and rheological properties of the latter.[38−44] As the PLC we have chosen PET/0.6PHB, where PET is poly(ethylene terephthalate), PHB is *p* -hydroxybenzoic acid, and 0.6 is the mole fraction of the LC constituent (PHB) in the copolymer. Our PLC is only one in a series of PET/*x*PHB copolymers; their phase diagram as a function of $x$ was already established[45] on the basis of results reported in 18 earlier publications. As for the EP, we have decided to use Bisphenol A polycarbonate (PC) since the phase diagram of PC + PET/0.6PHB blends is also known,[46] as well as their rheological properties up to 20 wt % of the PLC.[47]

## Experimental Section

**Materials and Their Preparation.** PET/0.6PHB was obtained from Eastman Kodak, Kingsport, TN, as well as from Unitika Ltd., Kyoto, Japan (LC-3000). PC was a Bisphenol A polycarbonate produced by Bayer AG, Leverkusen, Germany (Makrolon 2800). The former was well characterized in ref 45 (but see the beginning of the subsection Polymer Liquid Crystal (PET/0.6PHB) and the Blends below). As for the latter, its density is $\rho = 1.20$ g·cm$^{-3}$, melt flow index (MFI 300/11.8) = 7 g/10 min; stress at yield $\sigma_y = 65$ MPa; modulus of elasticity in tension $E = 2300$ MPa, and elongation at fracture $\epsilon_f = 110\%$. All samples we have studied, at any location, had the same basic thermal history, and no differences were found between the Eastman Kodak and Unitika samples of the PLC. To exclude possible degradation by hydration, the components were dried in a vacuum drier. Blending was done in Strasbourg in a single-screw Goettfert extruder with the length-to-diameter L/D ratio of 24. The extrusion temperatures were 230, 260, 270, and 280 °C; the screw speed gave the residence time of ∼3 min. The extruded rod with the diameter of ∼3 mm was granulated using a pelletizing unit. Samples for mechanical testing were prepared by injection molding under the following conditions: temperatures in the barrel, 270, 280, 290, and 300 °C; mold temperature, 100 °C; filling pressure, 130 MPa; packing pressure, 46 MPa; packing time, 10 s; cooling time in the mold, 15 s.

**Dynamic Mechanical Measurements (DMA).** The dynamic mechanical measurements were made using a computer-controlled free-oscillation torsion pendulum. The torsion pendulum test is standardized for plastics testing according to ISO 6721 (1992) part 2 or ASTM standard 2236-70. The construction used is similar to the so-called inverted type where the inertia element (disk) is suspended by a fine wire and a counterweight. The free damped torsional oscillation of the system consisting of the sample and the disk is monitored by an optical−electrical sensor which provides appropiate signals for measuring the oscillation frequency and the decay of amplitudes with a computer on-line. These input data (completed by the dimensions of the sample and the moment of inertia of the oscillating system) are instantly converted to the desired output data of the complex shear modulus.

The samples were in the form of strips, 60 mm long between the clamps, 10 mm wide, and 2 mm thick. To avoid orientational effects, the strips were always cut from the sheets along the processing direction. The measuring procedure started at a low temperature, and the oscillation experiment was initiated and repeated in steps of several degrees K while the sample was heated up continuously at the rate of 2 K/min. During the temperature scan from −185 to +185 °C, the frequency was adjusted so as to be nearly constant at about ∼1 Hz by changing the inertia disk in dependence on the shear storage modulus of the material.

**Dielectric Measurements.** The samples for the dielectric measurements were pressed by a Darragon press at 300 °C for 5 min, producing films with of 100 $\mu$m thickness. Silver electrodes with a 30 mm diameter were evaporated onto the samples. The isothermal dielectric behavior, characterized by the complex dielectric permittivity

$$\epsilon^*(f) = \epsilon'(f) - i\epsilon''(f) \tag{1}$$

(where $f$ is the frequency, $\epsilon'$ is the real part, $\epsilon''$ is the imaginary part, and $i = (-1)^{1/2}$ was measured in the frequency range from $10^{-2}$ to $10^6$ Hz using a Schlumberger frequency-response analyzer FRA 1260 supplemented by a buffer amplifier of variable gain.[48] The temperature of the sample was controlled by a custom-made nitrogen gas jet heating system covering a broad temperature range with the resolution of ± 0.02 K.

The data were quantitatively analyzed by fitting the model function of Havriliak and Negami (H−N)[49,52] to the isothermal relaxation curves. The H−N function reads

$$\epsilon'(f) - \epsilon_\infty = \frac{\Delta\epsilon}{(1 + (if/f_0)^\beta)^\gamma} \tag{2}$$

Here $\Delta\epsilon$ is the intensity, $f_0$ is a characteristic frequency nearly

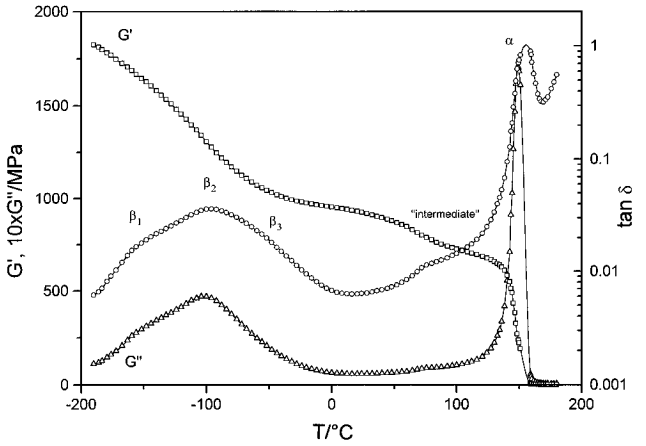


**Figure 1.** Shear storage modulus $G'$, shear loss modulus $G''$, and mechanical loss factor tan $\delta$ vs temperature for PC.

equal to the peak frequency $f_p$, $e_\infty = \epsilon'(f)$ for $f \gg f_p$, and $\beta$ and $\gamma$ are fractional shape parameters ($\beta$ is also used below for a relaxation label) related to the width and the asymmetry of the peak. As discussed also by Hartmann,[50,51] this generalization of the single relaxation time model by Hudson et al. combines the broadening of the Cole−Cole model with the asymmetry of the Davidson−Cole model. As described by Schlosser and Schönals,[52] eq 2 can be used to represent the isothermal data. There is also a capability of decomposing the whole relaxation curve into constituents corresponding to individual relaxation regions.[52,53]

## Mechanical Relaxations

**Polycarbonate.** A DMA scan for the pure polycarbonate is shown in Figure 1; the shear storage modulus $G'$, the shear loss modulus $G''$, and the mechanical loss factor tan $\delta$ are displayed as a function of temperature. The steps in $G'$ and the accompanying peaks in $G''$ and tan $\delta$ indicate three relaxation regions located respectively around −100, 75, and 148 °C. In this discussion, these relaxations will be referred to as the $\beta$, "intermediate" and $\alpha$ relaxation, respectively. The temperatures are taken from the peak positions of the $G''(T)$ function; tan $\delta$ peaks are typically found at somewhat higher temperatures depending on the intensity and/or width of the transition. This fact, as well as the frequency dependence of relaxational processes, should be taken into account when our results are compared with those of other sources. We note that the glass transition temperature of PC ($\alpha_{PC}$) agrees with the thermal mechanical analysis (TMA) result in ref 46. The literature contains extensive reports on the mechanisms of relaxations in polycarbonates; see refs 54−58 and references therein. Thus, Bendler and Shlesinger[55] discussed defect cluster formation during thermal quenching to temperatures below the glass transition temperature $T_g$. A relaxational process caused by pumping thermal energy into the system can result in the destruction of these defects, or their migration to the chain ends, or else as suggested by LeGrand and co-workers[56] in more homogenous distribution of the defects. Moreover, chain ends might be disentangled from other chain ends or segments. Jho and Yee,[57] who have performed DMA measurements on PC postulated the cooperative character of the $\beta$ process around −100 °C (in ref 57 this process is called $\gamma$). Their DMA results agree with ours in Figure 1, except that their lowest experimental temperature is −150 °C while ours is −185 °C, hence we see some additional features. Weigand and Spiess[58] explained their $^1$H NMR results in terms of methyl group rotations, large-amplitude phenyl flips, and main-chain wiggling. Keeping in mind these various proposed mechanisms, let us inspect Figure 1 in some more detail.

We observe that the broad $\beta$ relaxation constitutes in fact an overlap of three mechanisms, $\beta_1$−$\beta_3$ in the figure. $\beta_1$ appears to be the start of the defect migration; this is the process discussed by Bendler and Shlesinger[55] and LeGrand et al.[56] The large $\beta_2$ peak is the homogenization of the defects noted in refs 55 and 56; at the same time, this might well be the cooperative motion of Jho and Yee, as well as the main-chain wiggling of Weigand and Spiess.[59] The homogenization can deprive some atom groups of a fraction of the free volume $v^f$ they had at lower temperatures, which explains the decrease of $G''$ and tan $\delta$ beyond the peak maximum. The $\beta_3$ region, with its relatively stable $G'$, might be explained by the defect migration to the chain ends and subsequent *disentanglement* of the chain ends from other chain ends or segments envisaged by Bendler and Shlesinger. We recall the role of entanglements in smectic PLC phases discussed by Hudson and co-workers.[30] The "intermediate" process around + 75 °C, indicated by the weak shoulder in tan $\delta$ and the small step of $G'$, is discussed in more detail in the subsection Polycarbonate below; it has been known under that name since the 1960.[54] Then we have the $\alpha$ relaxation, which corresponds to the glass transition $T_g$ of PC at ∼148 °C when large-scale microbrownian movements become liberated and large-amplitude phenyl flips become possible. However, as discussed by Jho and Yee,[57] the orientation of the two phenylene planes in PC separated by the carbonate group may be either asymmetrically skewed to different directions or distorted to the same direction. The energy barrier between these two orientations is quite small,[61] hence they might coexist well also above $T_g$—and we are not far from the condis crystals of Wunderlich and co-workers[62,63] with their positional and orientational but not conformational order.

**Polymer Liquid Crystal (PET/0.6PHB) and the Blends.** For our pure PLC, that is PET/0.6PHB, DMA results have already been reported for identical samples in ref 45 at frequencies comparable to those in the present study. On the basis of these DMA and other results,[45] we recall that the PLC has the following: a $\beta$ relaxation centered at ∼−50 °C, with both PET and PHB constituents participating in the process,[64,65] and, with Chen and Zachmann,[66] suggesting for PET the onset of hindered rotations of the $CH_2$ groups combined perhaps with motions of COO groups; a transition which is the glass transition of the PET-rich or matrix phase at ∼+62 °C; an $\alpha'$ transition which starts at ∼80 °C and extends to 100 °C or so and constitutes cold crystallization of PET; the glass transition of the islands (= the PHB-rich phase) at ∼160 °C, comparable to that of pure PHB; melting at ∼199 °C, when the islands become a smectic E phase (as first established by Yoon and co-workers[67]) while the matrix becomes an isotropic melt; and subsequent transformations of the PHB-rich phase, smectic E → smectic B → isotropic liquid.

In Figure 2 we show the dependence of the loss modulus $G''$ on the temperature for blends containing 5, 10, 15, and 20 wt % PLC, and also for pure PC for comparison. The relaxation processes of the pure components are also found in the blends. In the high-temperature region, the glass transition peak of the PC ($\alpha_{PC}$) is dominant. While no remarkable effect on the peak height can be noticed, its temperature position is clearly influenced by the PLC fraction increasing from

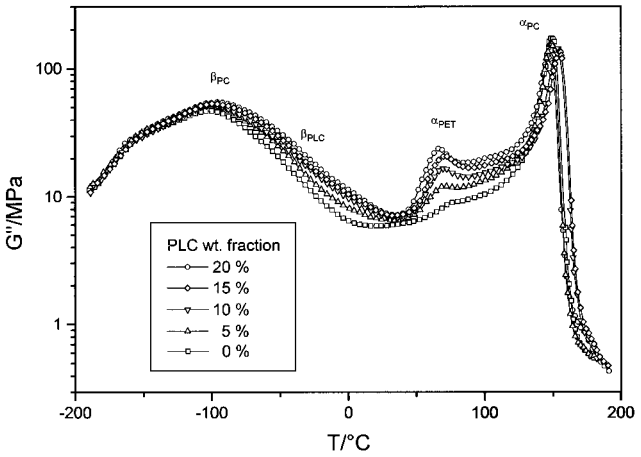


**Figure 2.** Shear loss modulus $G''$ vs temperature for PC + PLC blends.

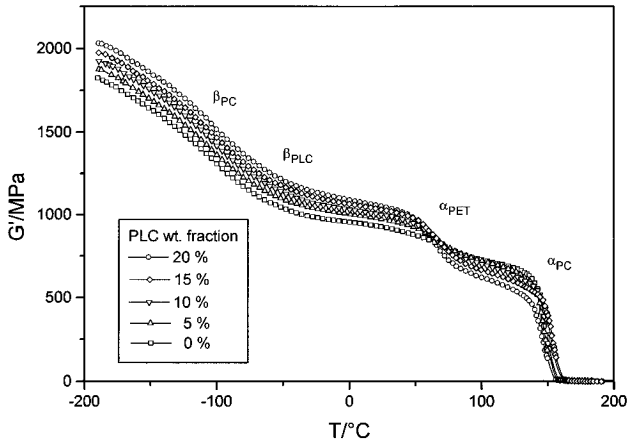


**Figure 3.** Shear storage modulus $G'$ vs temperature for PC + PLC blends.

148 (pure PC) to 154 °C for the 15% PLC blend and dropping to 147 °C for the 20% blend. The phase diagram for PC + PET/0.6PHB blends[46] indicates that the lowest PLC concentration $\theta_{\text{LC limit}}$ at which the LC-rich islands are formed is ∼15% PLC. The rheological results for the same blends[47] show that the $\theta_{\text{LC limit}}$ is between 15 and 20% PLC. This explains the lowering of the $\alpha_{PC}$ glass transition: liberated at 20% PLC from many of the perturbing PHB sequences, the PC-rich matrix virtually returns to the glass transition of pure PC. We are back to the approach of Surovtsev and coworkers in considering the minor blend component as a pertubation.[37] This is in spite of the fact that some PC chains apparently participate in the island formation (small partial miscibility of PC with PHB but none with PET), since the glass transition line of PC bifurcates at the $\theta_{\text{LC limit}}$.[46]

The glass transition α peak of the PET, located near to the intermediate relaxation shoulder of PC, increases in intensity with growing PLC fraction. There is a small but clear shift to higher temperatures of the combined ($\alpha_{PC}$ + intermediate PC) peak for up to 15% PLC, when that peak is observed at 70 °C, but its maximum goes down to 66 °C for 20% PLC. We know that the $\alpha_{PET}$ transition take place at 62 °C, hence increasing the PLC concentration moves the combined peak closer to that value. This happens until the $\theta_{\text{LC limit}}$ is reached above 15% PLC, the LC-rich island phase separates, and therefore, the peak moves back to a lower temperature. Another splitting up of $G''$ curves with increasing amount of PLC occurs in the region between the room temperature and −90 °C. There is no doubt that it is an effect of the $\beta_{PLC}$ relaxation overlaying with $\beta_{PC}$. The main peak $\beta_2$ of the latter at −100 °C is shifted monotonously to higher temperatures with increasing amounts of the PLC; the effect is more clearly demonstrated by the dielectric data below. Overall the mechanical loss modulus results for the PC + PLC blends are dominated by the phase separation, that is, by the island formation when the $\theta_{\text{LC limit}}$ is exceeded. Nevertheless, the shift of the dynamic glass transition $\alpha_{PC}$ found for PLC concentrations up to 15% is typical for morphological interactions inducing higher molecular order with subsequent restriction on the molecular mobility of one or both phases. Similar effects of composition-dependent mutual influence on the molecular order of the components were reported for polycarbonate + poly(ϵ-caprolactone) blends.[68]

The morphological characteristics of the blends deduced from the temperature dependence of the mechanical loss factor are also reflected in the shear storage modulus vs temperature curves shown in Figure 3. That plot clearly displays several regions, with three largest stepwise decreases of the materials stiffness caused by the relaxations $\beta_{PC}$, $\alpha_{PET}$, and $\alpha_{PC}$ (from low to high temperatures). The dependence of $G'$ on the PLC concentration varies with $T$. At temperatures below the dynamic glass transition of the PET component, the modulus increases with increasing concentration of the PLC. There is an inverse behavior above $\alpha_{PET}$ where the modulus decreases with increasing PLC concentration before the final drop connected with the $\alpha_{PC}$ and $\alpha_{PHB}$ transitions occurs. Once more, these findings clearly confirm the multiphase character of the blends. Obviously it is the special influence of the modulus level of the PLC and its temperature dependence that cause that inversion effect at $\alpha_{PET}$. Due to its high molecular order, even in the glassy state the PLC exhibits higher modulus than the PC. Therefore, acting as a dispersed phase, PLC enhances the modulus of the blends at lower temperatures. At $\alpha_{PET}$, the dynamic glass transition of PET brings its modulus level remarkably below that of the glassy PC matrix, thus inverting the order of the curves. The differences between the blends in the final modulus drops at ∼150 °C are in accordance with the phase structures and morphology already discussed in relation to the $\alpha_{PC}$ peak of the mechanical loss factor; once again the formation of the islands above the $\theta_{\text{LC limit}}$ manifests itself. We recall rule 4 of formation of hierarchical structures:[17] the structure of a smaller entity determines the structure of a larger entity.

## Dielectric Relaxations

**Polycarbonate.** In Figure 4 the logarithmic dielectric loss log $\epsilon''$ is plotted vs the temperature for several frequencies. As in the mechanical experiments, the dielectric spectra show two main relaxation regions. The dependence of the peak frequency $f_{p\beta}$ for the low-temperature $\beta$ relaxation on the temperature $T$ has the Arrhenius form

$$f_{p\beta} = f_{\beta\infty} \exp\left[-\frac{E_{A\beta}}{kT}\right] \tag{3}$$

where $f_{\beta\infty}$ is the preexponential factor and $E_{A\beta}$ is the activation energy. Locations of $f_{p\beta}$ are evaluated from the $\epsilon''$ values. The results for different compositions are shown in Figure 5. The results for pure PC can be

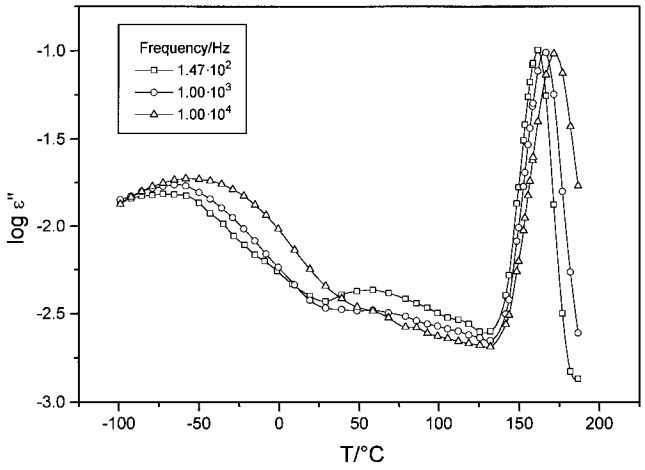


**Figure 4.** Logarithm of dielectric loss $\epsilon''$ vs temperature for PC at different frequencies.

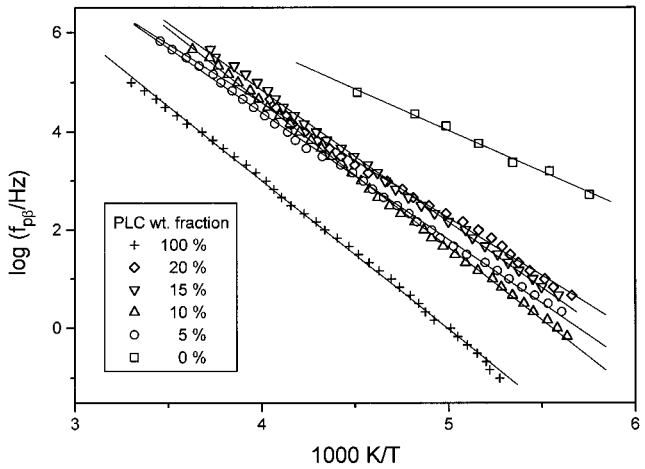


**Figure 5.** Arrhenius plot for the $\beta$ relaxation of PC in PC + PLC blends.

represented by eq 3 with log ($f_{\beta\infty}$/Hz) = 12.4 and $E_{A\beta}$ = 32.2 kJ·mol$^{-1}$.

The temperature dependence of a relaxation peak frequency can also be represented by the well-known empirical Vogel−Fulcher−Tammann−Hesse[69] (VFTH) equation

$$\log f_{p\beta} = \log_{\alpha\infty} - \frac{A}{T - T_0} \qquad (4)$$

in which $f_{\alpha\infty}$ and $A$ are constants and $T_0$ is the so-called ideal glass transition temperature. The last equation serves in principle also for other relaxations such as $\beta$. In the following we shall use both eqs 3 and 4.

The results for $f_{\beta\infty}$ calculated from eq 3 from $\epsilon''$ peaks are shown in Figure 5, while the respective parameters are listed in Table 1. Similar to the mechanical measurements, the dielectric experiments display the process located between $\beta$ and α relaxation. As noted above, this process has been known for decades. It has been found sensitive to thermal treatment of the sample; the intensity becomes reduced by annealing. It has been argued that this process is not a relaxation region in the classical sense related to the equilibrium structure of the polycarbonate but may be due to the relaxation of frozen-in stress. The intermediate region may be also related to the physical aging of the polymer in a similar way as discussed by Schönhals and Schröter.[70] To clarify the molecular mechanism of this process, some further investigations are necessary for samples with different thermal histories.

**Table 1. VFTH Parameters for the α Relaxations**

| sample | log ($f_{\alpha\infty}$/Hz) | $A$/K | $T_0$/K | ref |
|---|---|---|---|---|
| PET | 18.8 | 1269 | 288.5 | 52 |
| PET/0.6PHB α′ | 19.9 | 907 | 286 | 64 |
| PET/0.6PHB α | 17.4 | 1286 | 284 | 64 |
| PET/0.6PHB α | 17.9 | 722 | 295 | *a* |
| polycarbonate | 14 | 743 | 373.3 | *a* |
| blends | | | | |
| 05% PLC | 15 | 847 | 367 | *a* |
| 10% PLC | 15.2 | 888 | 364 | *a* |
| 15% PLC | 15.2 | 922 | 360 | *a* |
| 20% PLC | 15.1 | 926 | 357.3 | *a* |

[a] This work.

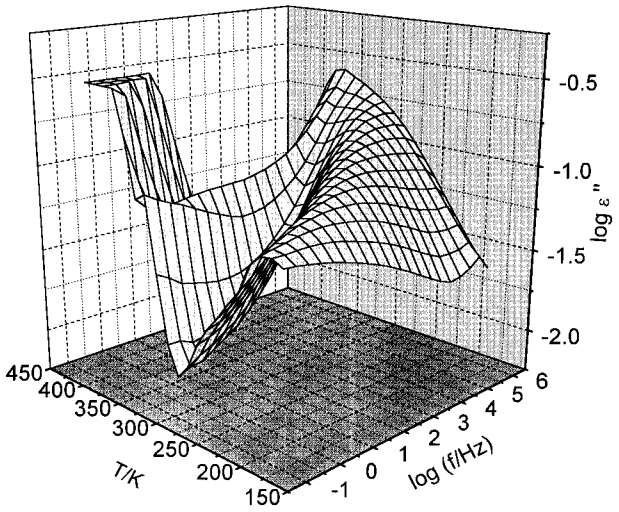


**Figure 6.** Logarithm of dielectric loss $\epsilon''$ vs temperature and logarithm of frequency for the sample PET/0.6PHB.

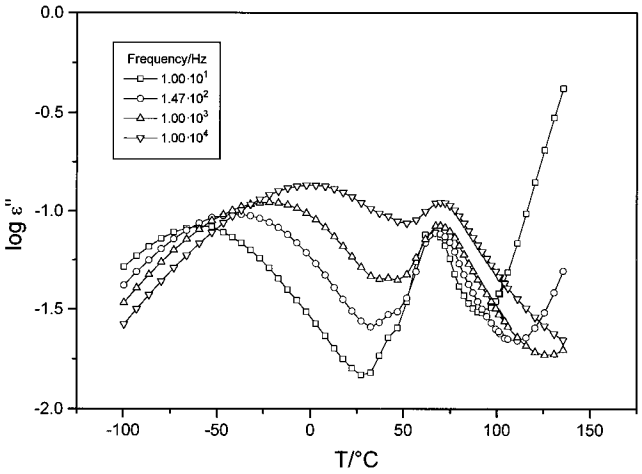


**Figure 7.** Logarithm of dielectric loss $\epsilon''$ vs temperature for the sample PET/0.6PHB at different frequencies.

**Polymer Liquid Crystal (PET/0.6PHB).** Dielectric relaxation studies of our PLC have been reported by Gedde et al.[64] and by Takase et al.[71] Figure 6 shows the dielectric loss $\epsilon''$ vs frequency and temperature for our sample. Confirming results in refs 64 and 71, two pronounced relaxation regions can be observed: the high-temperature α relaxation and the $\beta$ relaxation at lower temperatures. Figure 7, which shows temperature scans at fixed frequencies for our PLC, indicates that the $\beta$ relaxation is quite strong and quite broad as compared to the α relaxation. We would like to concentrate first on the former.

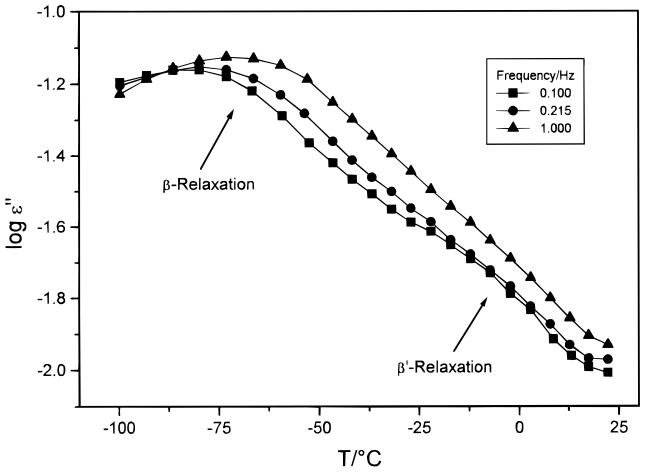


**Figure 8.** Logarithm of dielectric loss $\epsilon''$ vs temperature for PET/0.6PHB for different frequencies in the $\beta$ relaxation region, showing the $\beta'$ relaxation additional to the $\beta$ relaxation.

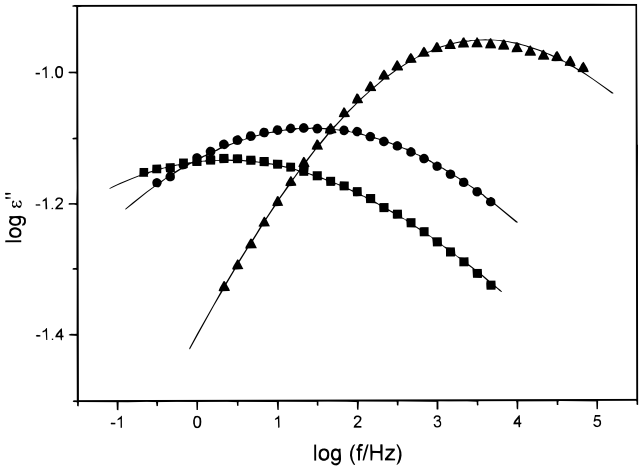


**Figure 9.** Representation of the dielectric $\beta$ relaxation of PET/0.6PHB by the H−N function: (■) $T = 193.5$ K, $\beta = 0.200$, $\gamma = 0.75$, $\Delta\epsilon = 1.026$, $\log f_0 = -0.27$; (●) $T = 206.8$ K, $\beta = 0.205$, $\gamma = 0.91$, $\Delta\epsilon = 1.044$, $\log f_0 = 1.22$; (▲) $T = 241.2$ K, $\beta = 0.281$, $\gamma = 0.60$, $\Delta\epsilon = 1.197$, $\log f_0 = 2.83$.

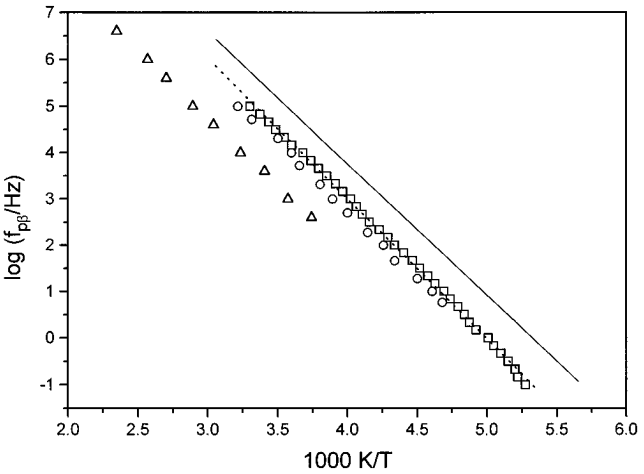


**Figure 10.** Arrhenius plot for the dielectric $\beta$ relaxation: (□) PET/0.6PHB; dotted line, fit of the Arrhenius equation to the data; (○) PET/0.8PHB from ref 64; (△) PHB from ref 73; solid line, Arrhenius fit to the $\beta$ relaxation data of amorphous PET taken from ref 72.

The relatively strong $\beta$ loss peak indicates that not only rotational fluctuations of the $CH_2$ groups, proposed as the molecular mechanism for this relaxation by Chen and Zachmann,[66] play a role. It appears that molecular motions of the COO groups contribute to the relaxational process in question.

A meticulous investigation at low frequencies shows that the $\beta$ relaxation region consists of two distinct processes (Figure 8). At low temperatures, a pronounced relaxation peak can be seen, which we shall continue to call $\beta$ relaxation.[64,65,71] This relaxation is followed by a second process at higher temperatures, much lower in intensity, not reported in earlier work. The reason may be that in our study a broad frequency range is covered, including low frequencies. We shall name this process $\beta'$ relaxation. Unfortunately, this relaxation occurs only as a weak shoulder on the high-temperature side of the $\beta$ relaxation, hence it cannot be analyzed with regard to relaxation rates or intensities. Moreover, with increasing frequency the $\beta$ peak covers the $\beta'$ relaxation quite rapidly. Gedde and his colleagues[64] noted that the difference between the relaxed and unrelaxed dielectric constants is for PET/xPHB copolymers (for pure copolymers $\theta = x$) independent of composition—which means that both PET and PHB participate in the relaxation. Since we have multiple evidence that PET/0.6PHB forms the PET-rich matrix plus PHB-rich islands, the $\beta$ and $\beta'$ relaxations might be caused respectively by these two phases; see a further discussion below.

The H−N function, eq 2, has beeen used to represent the $\beta$ relaxation results. Figure 9 shows the calculated (continuous line) and experimental (various symbols) values of the dielectric loss $\epsilon''$. Clearly the H−N function serves very well. The relaxation rate $f_{p\beta}$ is well represented by the Arrhenius formula, eq 3, with $\log (f_{\beta\infty}/\text{Hz}) = 15.9$ and $E_{A\beta} = 57.8$ kJ·mol$^{-1}$; the quality of the fit is demonstrated in Figure 10. Our value of $E_{A\beta}$ is quite close to that of Gedde and co-workers,[64] namely, 56 kJ·mol$^{-1}$.

To discuss the mechanism of the $\beta$ relaxation in our copolyester, the data for it are compared with those for the amorphous PET[72] and pure PHB[73] in Figure 10. The figure shows that the $\beta$ relaxation rates for PET/0.6PHB lie between those of PET and PHB. This means, first, that both ethylene terephthalate (ETP) and hydroxybenzoic acid (HBA) units contribute simultanously to that process—as already concluded by Gedde et al. and noted above. Second, with increasing HBA (=PHB) contents, the $\beta$ relaxation is shifted to higher temperatures—as can bee seen in the figure for PET/0.6PHB and for PET/0.8PHB results from ref 64. On this basis one can speculate on the molecular character of the $\beta'$ relaxation. Remembering the two-phase morphology, the $\beta'$ relaxation can be understood as a process that occurs in the islands since it becomes active at higher temperatures than the $\beta$ relaxation. Assuming that PET and PHB units have dipole moments of comparable magnitude, from the comparison of the intensities of the $\beta$ and the $\beta'$ relaxation one infers that PET-rich areas must be larger than the PHB-rich islands. This of course confirms what has been already seen in SEM[5] and further confirmed by wide-angle X-ray scattering (WAXS).[17] Both SEM and WAXS results show that the islands constitute a minor fraction of the total volume of the PET/0.6PHB material. We recall rule 5 of formation of hierarchical structures:[17] assembling entities in a specified way can achieve properties that a system of *unassembled* entities does not have. In our case, chemically speaking, PHB is the major component in the copolymer. However, it takes a high *local* concentration of PHB sequences—and a favorable topo-

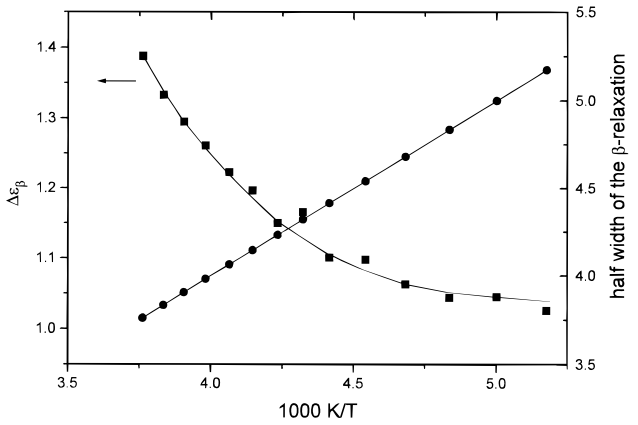


**Figure 11.** Intensity (■) and half-width (●) of the dielectric $\beta$ relaxation. Lines are guides for the eyes.

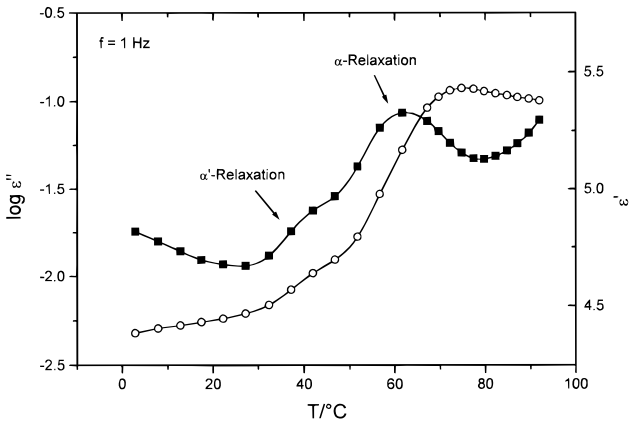


**Figure 12.** Logarithm of dielectric loss $\epsilon''$ vs temperature at 1 Hz for PET/0.6PHB showing the α and the α′ relaxations.

logical arrangement (low degree of entanglements)—to create an island. In such a way, our interpretation of the origin of the $\beta'$ relaxation acquires a base consistent with concepts of hierarchy formation and with experiments of several kinds.

Figure 11 gives the temperature dependencies of the half-width $b$ and of the relaxation strength $\Delta\epsilon_\beta$ of the $\beta$ peak. As is known for the most amorphous polymers, $\Delta\epsilon_\beta$ increases with increasing temperature. This can be explained by increases with temperature of the fluctuation angle of the dipole component (which is related to the $\beta$ relaxation) and/or the number of dipoles that contribute to the process. In distinction to ref 64 we have found that the $\beta$ peak is asymmetric (see Figure 8), but since that peak is very broad, the difference may be due again to a wider frequency range in our study. As Figure 11 shows, the half-width of the peak decreases with increasing temperature. The width of a $\beta$ process peak is often attributed to a distribution of relaxation times, due in turn to a distribution of molecular environments of the moving unit. Adopting this point of view, one can conclude that the width of the distribution of different environments decreases with increasing temperature.

Focus now on the α transition region of the PET/0.6PHB. A closer inspection of this zone shows that that zone is also split into two relaxation regions; see Figure 12. A relaxation peak with a small relaxation strength can be identified at lower temperatures; we shall call it α′. It is followed by the $\alpha_{PET}$ glass transition peak with a considerably higher intensity at higher temperatures. Unfortunately, the α′ process could not be better quantified for several reasons. First, it appears only as a

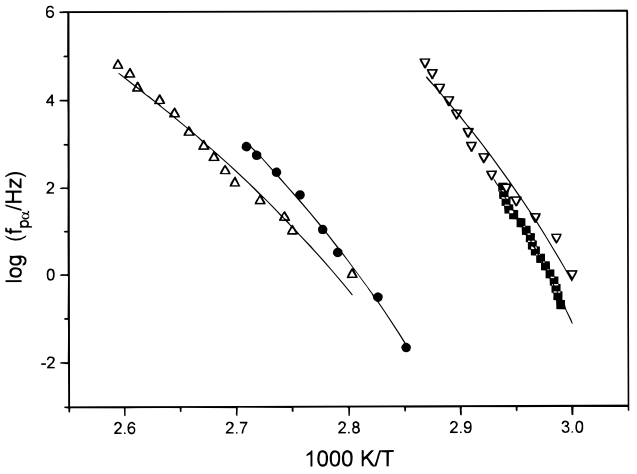


**Figure 13.** Arrhenius plot for the dielectric α relaxation of PET/0.6PHB: (■) α relaxation, this study: (▽) α′ relaxation; (△) α relaxation from ref 64; (●) α relaxation of PET from ref 52; lines are fits of the VFTH eq 4 to the data.

low-temperature shoulder of the α process and is badly resolved. Second, the $\beta$ relaxation, which is considerably more intensive, moves into the α transition zone and covers the α′ relaxation at higher temperatures. However, see a discussion of $\beta'$ below. Figure 13 gives the relaxation map for the α relaxation. We have also included in Figure 13 the data for the α process taken from ref 64 and the data for amorphous PET from ref 51. All the data can be approximately described by the VFTH equation; see lines in Figure 13. Parameters of eq 4 for all materials studied are listed in Table 1.

Figure 13 shows that the α process of PET in the PLC occurs at lower temperatures than the α relaxation in amorphous PET. As pointed out already, the α′ process occurs at even lower temperatures than the α relaxation. The lowering of the glass transition temperature in the PLC compared with that of amorphous PET, also found in ref 64, is surprising at first glance because the copolymerization of PET-type with PHB-type units introduces relatively inflexible PHB segments into the system, hence the glass transition temperature should increase. However, the rodlike PHB units can prevent the densest packing otherwise possible in the system. Thus, the copolymerization introduces an additional amount of free volume which causes *plasticizition* of the system and lowers the glass transition temperature. With this simple model, the glass transition temperature of PET/*x*PHB can be understood as a competition of chain stiffness and introduction of an additional amount of $v^f$—both due to the copolymerization.

The appearance of α′ and α relaxation processes will now be reconsidered in the framework of the two-phase structure of PET/*x*PHB. Assume that the low-temperature α′ process is assigned to a relaxation transition in HBA (=PHB)-rich domains while we already know that the high-temperature α process constitutes the glass transition in PET-rich domains.

Such an assignment can be justified by two arguments. First, the $\beta'$ relaxation process was related by completely different arguments to the PHB-rich islands. We remember that the $\beta'$ relaxation has much lower intensity than the $\beta$ relaxation of the PET-rich matrix. Since the α′ relaxation has lower dielectric relaxation strength than the α relaxation, it seems plausible to relate this relaxation process to the islands. Second, in comparison the α relaxation, the α′ relaxation is shifted to lower temperatures—which was explained by

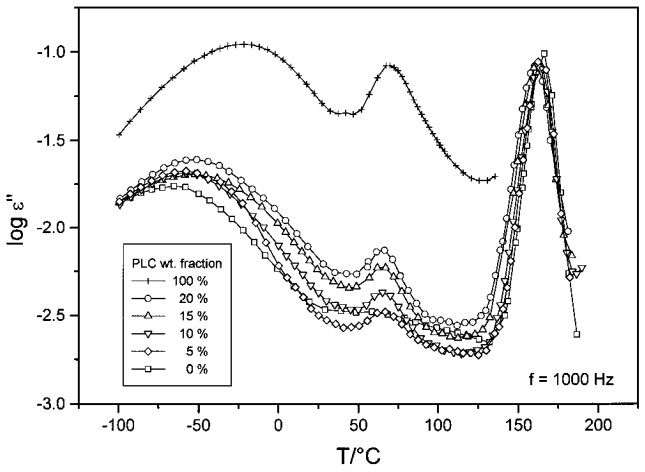


**Figure 14.** Logarithm of dielectric loss $\epsilon''$ vs temperature for PC + PLC blends at 1000 Hz.

**Table 2. Parameters of the Arrhenius Equation for the $\beta$ Relaxation of Polycarbonate**

| wt % PLC | $\log(f_{\beta\infty}/\text{Hz})$ | $E_{A\beta}/(\text{kJ·mol}^{-1})$ |
|---|---|---|
| 0 | 12.42 | 32.12 |
| 5 | 13.98 | 44.79 |
| 10 | 15.57 | 51.34 |
| 15 | 16.4 | 56.51 |
| 20 | 14.75 | 49.58 |
| 100 | 15.9 | 57.8 |

a higher degree of internal plasticization. The $\beta'$ relaxation, also related to the islands, is shifted simultaneously to higher temperatures in comparison to the $\beta$ relaxation. Such shifts upward of the low-$T$ relaxation and downward of the high-$T$ relaxation have been found before for polymers plasticized with low molecular weight plasticizers.[74]

**Polycarbonate + PLC Blends.** Figure 14 shows the dielectric behavior for the both pure materials and their blends with different PLC concentrations (5, 10, 15, and 20 wt %) at a frequency of 1 kHz vs temperature. The α relaxation of PET can be identified easily; its strength increases with increasing concentration of the PLC. As in the mechanical case, this result indicates a very well separated two-phase structure of the blends.

Consider first the low-temperature relaxation region. Given the two-phase structure, we would expect to see the $\beta$ peak of the PLC. It is indeed very visible, but with a partial overlap with the $\beta$ relaxations of PC, the $\beta_3$ relaxation is particular. We recall that we have already shown in Figure 5 the temperature dependence of the $\beta$ relaxation rates of polycarbonate analyzed in terms of the Arrhenius eq 3. The respective preexponential factors and the activation energies are listed in Table 2. For low concentrations of the PLC both quantities increase at first, display a local maximum at 15%, and after crossing the $\theta_{\text{LC limit}}$, they both decrease. A natural explanation is that—as we have argued before—gradual addition of the PLC results in perturbation of the PC structure. Since PET is comparable in its flexibility to the PC matrix, the perturbation is caused mainly by the relatively rigid PHB component of the PLC. Therefore, the perturbation increases at first, but it decreases above the $\theta_{\text{LC limit}}$ when the PHB-rich islands are formed. There are some indications for such an interpretation from ultrasonic and spectroscopic investigations.[75] At the same time, while our interpretations above in terms of the island formation are on firm ground, exceptionally in the case of the parameters in Table 2 that explanation is only tentative, this

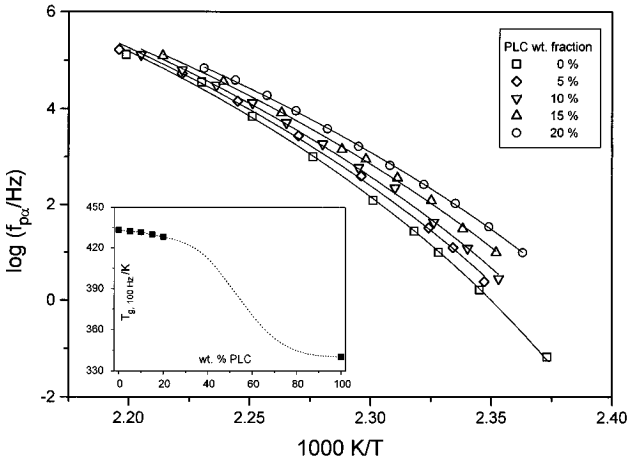


**Figure 15.** Arrhenius plot for the dielectric α relaxations of PC + PLC blends (inset: dynamic glass transition temperature vs composition).

because of the already mentioned overlap of the $\beta_3$ relaxation of PC with the $\beta$ relaxation of the PLC.

The temperature dependence of the α relaxation rates of PC displays the well-known VFTH behavior (eq 4) shown in Figure 15. The respective parameters are listed in Table 1. The temperature position of the α relaxation of PC at a fixed frequency shifts with increasing concentration of PLC to lower temperatures. We recall the partial miscibility of PC with PLC established in ref 46 and already referred to above. This interpretation is supported further by the observed broadening of the α peak with increasing PLC content characteristic for blend systems. Once again, a variety of results obtained by different techniques leads to a single interpretation. The dynamic glass transition temperature of PC can be calculated for 10 Hz with the help of the VFTH fits and plotted vs the PLC concentration; see the inset in Figure 15. The glass transition of the PET constituent of the PLC is also shown at the far right end. The result is essentially a step function, confirming once again that only a small part of the PLC is dissolved in the polycarbonate matrix.

**Acknowledgment.** Partial financial support for this work was provided by the Robert A. Welch Foundation, Houston (Grant B-1203). We appreciate discussions with Dr. Nandika Anne D'Souza, University of North Texas (UNT); Dr. Monika Plass, formerly at UNT and now at the Martin Luther University of Halle-Wittenberg; Prof. Jürgen Springer of the Technical University of Berlin; and Prof. Janusz Walasek of the Technical University of Radom. A reviewer provided helpful remarks.

## References and Notes

(1) Ferry, J. D. *Viscoelastic Properties of Polymers*, 3rd ed.; Wiley: New York, Chichester, 1980.
(2) Privalko, V. P.; Novikov, V. V. *The Science of Heterogeneous Polymers;* Wiley: Chichester, New York, 1995.
(3) Menczel, J.; Wunderlich, B. *J. Polym. Sci. Phys.* **1980**, *18*, 1433.
(4) Menczel, J.; Wunderlich, B. *Polymer* **1981**, *22*, 778.
(5) Brostow, W.; Dziemianowicz, T. S.; Romanski, J.; Werber, W. *Polym. Eng. Sci.* **1988**, *28*, 785.
(6) Flory, P. J. *Proc. R. Soc. A* **1956**, *234*, 60, 73.
(7) Abe, A.; Flory, P. J. *Macromolecules* **1978**, *11*, 1122.
(8) Flory, P. J.; Ronca, G. *Mol. Cryst. Liq. Cryst.* **1979**, *54*, 289, 311.
(9) Matheson, R. R., Jr.; Flory, P. J. *Macromolecules* **1981**, *14*, 954.
(10) Matheson, R. R., Jr.; *Macromolecules* **1986**, *19*, 1286.

(11) Jonah, D. A.; Brostow, W.; Hess, M. *Macromolecules* **1993**, *26*, 76.
(12) Blonski, S.; Brostow, W.; Jonah, D. A.; Hess, M. *Macromolecules* **1993**, *26*, 84.
(13) Brostow, W.; Walasek, J. *Macromolecules* **1994**, *27*, 2923.
(14) Sawyer, L. C.; Jaffe, M. J. *Mater. Sci.* **1986**, *21*, 1897.
(15) Sawyer, L. C.; Chen, R. T.; Jamieson, M. G.; Musselman, I. H.; Russell. P. E. *J. Mater. Sci. Lett.* **1992**, *11*, 69.
(16) Sawyer, L. C.; Jaffe, M. *Mater. Res. Soc. Symp.* **1992**, *255*, 75.
(17) Brostow, W.; Hess, M. *Mater. Res. Soc. Symp.* **1992**, *255*, 57.
(18) Tiller, A. R. *Macromolecules* **1992**, *25*, 4605.
(19) Brostow, W.; Kubát, J. *Phys. Rev. B* **1993**, *47*, 7659.
(20) Brostow, W.; Kubát, J.; Kubát, M. J. *Mater. Res. Soc. Symp.* **1994**, *321*, 99.
(21) Blonski, S.; Brostow, W.; Kubát, J. *Phys. Rev. B* **1994**, *49*, 6494.
(22) Kubát, J. *Phys. Status Solidi B* **1982**, *111*, 599.
(23) Kubát, J.; Rigdahl, M. In *Failure of Plastics;* Brostow, W., Corneliussen, R. D., Eds.; Hanser: Munich, Vienna, New York, 1986; Chapter 4.
(24) Blonski, S.; Brostow, W. *J. Chem. Phys.* **1991**, *95*, 2890.
(25) Brostow, W. *Kunststoffe* **1988**, *78*, 411.
(26) Brostow, W. *Polymer* **1990**, *31*, 979.
(27) Hudson, S. D.; Lovinger, A. J. *Polymer* **1993**. *34*, 1123.
(28) Hudson, S. D.; Lovinger, A. J.; Larson, R. G.; Davis, D. D.; Garay, R. O; Fujishiro, K. *Macromolecules* **1993**, *26*, 5643.
(29) Hudson, S. D.; Lovinger, A. J.; Venkataraman, S. K.; Liu, C.; Manzione, L. T. *Polym. Eng. Sci.* **1994**, *34*, 1327.
(30) Hudson, S. D.; Lovinger, A. J.; Gomez, M. A.; Lorente, J.; Marco, C.; Fatou, J. G. *Macromolecules* **1994**, *27*, 3357.
(31) Samulski, E. T. *Faraday Discuss.* **1985**, *79*, 7.
(32) Beery, D.; Kenig, S.; Siegmann, A.; Narkis, M. *Polym. Eng. Sci.* **1993**, *33*, 1548.
(33) Cheng, S. D. Z.; Janimak, J. J.; Sridhar, K.; Harris, F. W. *Polymer* **1989**, *30*, 494.
(34) Kühnpast, K.; Springer, J.; Scherowsky, G.; Giesselmann, F.; Zugenmaier, P. *Liq. Cryst.* **1993**, *14*, 861.
(35) Davidson, P.; Kühnpast, K.; Springer, J.; Scherowsky, G. *Liq. Cryst.* **1993**, *14*, 901.
(36) Wolff, D.; Cackovic, H.; Krüger, H.; Rübner, J.; Springer, J. *Liq. Cryst.* **1993**, *14*, 917.
(37) Surovtsev, V. I.; Vilenskii, V. A.; Zelenskaya-Surovtseva, N. M.; Bezuglaya, T. N. *Vysokomol. Soed. A* **1995**, *37*, 822 (*Polym. Sci. A* **1995**, *37*, 544).
(38) Huh, W.; Weiss, R. A.; Nicolais, L. *Polym. Eng. Sci.* **1983**, *23*, 779.
(39) Siegmann, A., Dagan, A.; Kenig, S. *Polymer* **1985**, *26*, 1325.
(40) Kiss, G. *Polym. Eng. Sci.* **1987**, *27*, 410.
(41) Groeninckx, G.; Crevecoeur, G. Bull. *Soc. Chim. Belg.* **1990**, *99*, 1031.
(42) Groeninckx, G.; Crevecoeur, G. *Polym. Eng. Sci.***1990**, *30*, 532.
(43) Lee, W.-C.; DiBenedetto, A. T. *Polym. Eng. Sci.* **1992**, *32*, 400.
(44) Michaeli, W.; Brinkmann, T.; Heidemeyer, P.; Höck, P; Witte, S. *Kunststoffe* **1992**, *82*, 1136.
(45) Brostow, W.; Hess, M.; Lopez, B. L. *Macromolecules* **1994**, *27*, 2262.
(46) Brostow, W.; Hess, M.; Lopez, B. L.; Sterzynski, T. *Polymer* **1996**, *37*, 1551.
(47) Brostow, W.; Sterzynski, T.; Triouleyre, S. *Polymer* **1996**, *37*, 1561.
(48) Kremer, F.; Boese, D.; Meier, Fischer, E. W. *Prog. Colloid Polym. Sci.* **1989**, *80*, 129. Pugh, J.; Ryan, T. *IEE Conf. Dielectr. Mater. Measure. Appl.* **1979**, *177*, 404.
(49) Havriliak, S.; Negami S. *J. Polym. Sci. C* **1966**, 14, 99.
(50) Hartmann, B.; Lee, G. F. *Proc. Int. Congr. Rheol.* **1988**, *10*−*1*, 392.
(51) Hartmann, B.; Lee, G. F. *J. Non-Cryst. Solids* **1991**, *131*−*133*, 887. Hartmann, B.; Lee, G. F.; Lee, J. D. *J. Acoust. Soc. Am.* **1994**, *95*, 226.
(52) Schlosser, E.; Schönhals, A. *Colloid Polym. Sci.* **1989**, *267*, 963.
(53) Schlosser, E.; Schönhals, A.; Carius, H.-E.; Goering, H. *Macromolecules* **1993**, *26*, 6027.
(54) McCrum, N. G.; Read, B. E.; Williams, G. *Anelastic and Dielectric Effects in Polymeric Solids*; Wiley: New York, 1967; Dover Publications: Mineola, NY, 1991.
(55) Bendler, J. T.; Shlesinger, M. F. *J. Mol. Liquids* **1987**, *36*, 37.
(56) LeGrand, D. G.; Olszewski, W. V.; Bendler, J. T. *Thermochim. Acta* **1990**, *166*, 105.
(57) Jho, J. Y.; Yee, A. F. *Macromolecules* **1991**, *24*, 1905.
(58) Weigand, F.; Spiess, H. W. *Macromolecules* **1995**, *28*, 6361.
(59) Jho and Yee[57] do not quote the work of Bendler, Schlesinger, and co-workers[55,56]. Weigand and Spiess[58] do not quote refs 55−57. Taking into account differences in approaches and terminology, it appears that each of the three groups has envisaged basically the same process independently from others.
(60) Brostow, W. *Polymer* **1980**, *21*, 1410.
(61) Bicerano, J.; Clark, H. A. *Macromolesules* **1988**, *21*, 585.
(62) Wunderlich, B.; Grebowicz, J. *Adv. Polym. Sci.* **1984**, *60/61*, *1*.
(63) Wunderlich, B.; Möller, M.; Grebowicz, J.; Baur, H. *Adv. Polym. Sci.* **1988**, *87*, 1.
(64) Gedde, U. W.; Buerger, D.; Boyd, R. H. *Macromolecules* **1987**, *20*, 988.
(65) Brostow, W.; Samatowicz, D. *Polym. Eng. Sci.* **1993**, *33*, 581.
(66) Chen. D.; Zachmann, H. G. *Polymer* **1991**, *32*, 1612.
(67) Yoon, D. Y.; Maschiochi, N.; Depero, L. E.; Viney, C.; Parrish, W. *Macromolecules* **1990**, *23*, 1793.
(68) Cheung, Y. W.; Stein, R. S. *Macromolecules* **1994**, *27*, 2512.
(69) Vogel, H. *Phys. Z.* **1921**, *22*, 645. Fulcher, G. S. *J. Am. Ceram. Soc.* **1925**, *8*, 339. Tammann, G.; Hesse, W. *Z. Anorg. Allg. Chem.* **1926**, *156*, 245.
(70) Schönhals, A.; Schröter, K. *Acta Polym.* **1986**, *37*, 453.
(71) Takase, Y.; Mitchell, R. G.; Odayima, A. *Polym. Commun.*, **1986**, ***27***, 76.
(72) Coburn, J.; Boyd, R. H. *Macromolecules* **1986**, *19*, 2238.
(73) Kalika, D.; Yoon, D. *Macromolecules* **1991**, *24*, 3404.
(74) Greiner, B. Doctoral Dissertation, Technische Hochschule für Chemie "Carl Schorlemmer", Merseburg, 1985.
(75) Plass, M., personal communication, 1995.

MA951706U